

Graphene-Based Conducting Inks for Direct Inkjet Printing of Flexible Conductive Patterns and Their Applications in Electric Circuits and Chemical Sensors

Lu Huang, Yi Huang (✉), Jiajie Liang, Xiangjian Wan, and Yongsheng Chen (✉)

Key Laboratory of Functional Polymer Materials and Center for Nanoscale Science & Technology, Institute of Polymer Chemistry, College of Chemistry, Nankai University, Tianjin 300071, China

Received: 27 November 2010 / Revised: 4 March 2011 / Accepted: 4 March 2011

© Tsinghua University Press and Springer-Verlag Berlin Heidelberg 2011

ABSTRACT

A series of inkjet printing processes have been studied using graphene-based inks. Under optimized conditions, using water-soluble single-layered graphene oxide (GO) and few-layered graphene oxide (FGO), various high image quality patterns could be printed on diverse flexible substrates, including paper, poly(ethylene terephthalate) (PET) and polyimide (PI), with a simple and low-cost inkjet printing technique. The graphene-based patterns printed on plastic substrates demonstrated a high electrical conductivity after thermal reduction, and more importantly, they retained the same conductivity over severe bending cycles. Accordingly, flexible electric circuits and a hydrogen peroxide chemical sensor were fabricated and showed excellent performances, demonstrating the applications of this simple and practical inkjet printing technique using graphene inks. The results show that graphene materials—which can be easily produced on a large scale and possess outstanding electronic properties—have great potential for the convenient fabrication of flexible and low-cost graphene-based electronic devices, by using a simple inkjet printing technique.

KEYWORDS

Flexible, inkjet printing, solution-processed, graphene, conductive patterns, applications

1. Introduction

Printing techniques, such as inkjet printing, are competitive alternatives to conventional photolithography for the production of electronic devices with advantages including low cost, ease of mass production, and flexibility [1, 2]. Compared with other printing techniques (e.g., screen printing and microcontact printing), inkjet printing has attracted more attention due to its significant advantages involving compatibility with various substrates, availability of non-contact and

no-mask patterning, low temperature processing, and no requirement for vacuum processing. As printable conducting inks, several conventional materials, such as metals and conductive polymers, have been widely studied. However, though the merits of these materials are significant, they still have some serious shortcomings. For example, metals like Au [3], Ag [4–6], and Cu [7] possess outstanding conductivities, but Au and Ag are too expensive to be used in large quantities while Cu is easily oxidized. Conducting polymers [8] have advantages for flexible displays,

Address correspondence to Yongsheng Chen, yschen99@nankai.edu.cn; Yi Huang, yihuang@nankai.edu.cn



but their applications are highly restricted by their relatively low conductivity, and poor thermal and chemical stability. Recently, carbon nanotubes (CNTs) have also been widely studied as conducting materials for printable inks [9–16]. Nevertheless, the poor dispersibility of CNTs has limited their applications, including for conducting inks. Obviously, there is still a need to find a better candidate for printable conducting inks.

Graphene, a one-atom-thick two-dimensional (2D) single layer of sp^2 -bound carbon, exhibits remarkable electronic and mechanical properties [17–19]. Due to these unique properties, graphene is expected to have plentiful applications in various technological fields, such as supercapacitors [20, 21], field-effect transistors (FETs) [22, 23], organic photovoltaics (OPVs) [24–28], sensors [29–32], and light-emitting diodes (LEDs) [33]. For solution-processing based applications, graphene oxide materials—which can be synthesized on a large scale by the modified Hummer's method—can be easily dispersed in water. More importantly, intrinsic structure and excellent electrical conductivity of graphene can be largely restored by the chemical or thermal reduction of these graphene oxide materials. Based on these properties, water-dispersible graphene materials can be used for many solution-processing based applications including, FETs, OPVs, LEDs and sensors by using the inkjet printing technique. Indeed, inkjet printing technique for FETs and gas sensors has been reported recently using graphene as the base material [34, 35].

In this paper, a series of studies of the inkjet printing parameters are presented using two types of graphene materials, namely single-layered graphene oxide (GO) and few-layered graphene oxide (FGO), and then various high image quality patterns with controllable line-width and thickness are prepared on different commercial flexible substrates by the direct inkjet printing method using aqueous solutions of these two graphene materials. Furthermore, using this simple technique, we have fabricated flexible electronic circuits and a novel enzyme-free electrochemical hydrogen peroxide (H_2O_2) sensor. Their attractive properties, combined with the ease of preparation and solution-processing capability, indicate that our flexible, low-cost, inkjet printed graphene-based

technique may have great potential applications in electronic circuits, detectors, and electronic devices such as FETs, LEDs and OPVs.

2. Experimental

2.1 Materials

Graphite (average particle diameter of 44 μm , 99.95% purity) was obtained from Qingdao Tianhe Graphite Co. Ltd. Polyethyleneimine (PEI, $M_w = 70\,000$ g/mol, 30 wt%) and ferrocene (Fc, 99% purity) were purchased from Alfa Aesar. Poly(sodium 4-styrene sulfonate) (PSS, $M_w = 10\,000$ g/mol, 25 wt%) was obtained from Zhichuan Yaodong Chemical Co. Ltd. H_2O_2 (30 wt%) was obtained from Tianjin Ruijinte Chemical Co. Polyimide (PI) was bought from Guangdong Xiangguan Electronic Material Co. Ltd and poly(ethylene terephthalate) (PET) was bought from Bayer Material Science Trading Co. Ltd.

2.2 Instrumentation

The viscosity of the prepared inks was measured by an Ubbelohde viscosity meter. Typical tapping-mode atomic force microscopy (AFM) measurements were performed using a Multimode SPM from Digital Instruments with a Nanoscope IIIa Controller. The contact angles of the GO solution on different substrates were measured by a JY-82 contact angle goniometer. The morphologies of the inkjet printed patterns were examined by a JEOL JSM-6700F scanning electron microscope (SEM). The concentrations of the prepared inks were determined by UV–vis spectroscopy (V-570 G-SCO). A semiconductor parametric analyzer (Keithley 4200, Keithley Instruments Inc., Cleveland, OH) was used to examine the resistance of the reduced patterns. Thermal gravimetric analysis (TGA) was carried out using a NETZSCH STA 409PC thermal analyzer. Cyclic voltammetry measurements were performed using a conventional three-electrode cell in a microcomputer-based electrochemical analyzer (Lanlike Co. Ltd., LK98BII).

2.3 Preparation of graphene inks

Graphene materials (GO and FGO) were synthesized by oxidation of graphite with a modified Hummers'

method [36–41]. The printable graphene-based inks were prepared by sonicating 150 mg of GO or 120 mg of FGO in 15 mL of deionized water for 2 h. After sonication, the dispersed solutions were centrifuged at 6000 rpm for 15 min to remove large-sized particles of graphene material. Then, the residual suspension was filtered through a filter with 0.45- μm pore size. The concentration of the filtrations was determined by UV–vis spectroscopy. Finally, the filtrations were diluted to the required concentrations (GO ink: 9 mg/mL, FGO ink: 5 mg/mL) by adding deionized water to obtain the stable and homogeneous graphene-based inks (Fig. S-1 in the Electronic Supplementary Material (ESM)).

2.4 Substrate treatment

To improve the wetting properties of organic substrates such as PET and PI, polyelectrolyte PSS (30 mg/mL) and PEI (13.5 mg/mL) solutions were prepared and used in a 0.5 mol/L NaCl aqueous solution. The PI substrates (30 mm \times 30 mm) were cleaned by sonication for 15 min in detergent, deionized water and acetone. PET was cleaned similarly but with ethanol replacing acetone. All the cleaned substrates were dried by pressurized nitrogen. Cleaned PI or PET was first submerged into the PSS solution for 20 min, then thoroughly rinsed with water and dried under compressed nitrogen, and then dipped into PEI solution for another 20 min, followed by water rinsing and nitrogen drying. This process creates two layers which consist of one layer of PSS and one layer of PEI.

2.5 Inkjet printing

Inkjet printing was carried out with a standard commercial office Hewlett-Packard Deskjet K7108 printer at room temperature. The prepared ink was injected into a cleaned HP 853 ink cartridge by a syringe. Before printing, the ink cartridge was allowed to stand for several minutes to ensure the ink was equilibrated in the cartridge, and then the patterns designed by Microsoft Powerpoint were printed onto the desired flexible substrates including normal printing paper, PET, and PI.

2.6 Reduction of printed patterns

The patterns printed on PI were heated to 400 °C at

3 °C/min and held at this temperature for 3 h in a mixture of 95 vol% argon and 5 vol% hydrogen under ambient pressure to restore their electrical properties. For the PET substrate, a lower annealing temperature was used.

2.7 Preparation of electrochemical H₂O₂ sensor

First, a graphene-based electrode was fabricated as above using inkjet printing and annealing in Ar/H₂ and used as the working electrode, together with a Pt electrode and an Ag/AgCl electrode to form the electrochemical sensor system. To make a graphene electrode as the working electrode as a sensor for H₂O₂ detection, Fc was used to modify the electrode as follows: Reduced graphene oxide (RGO, 2 mg), prepared using a similar method to that reported by Ruoff [42], was first functionalized with Fc (20 mmol/L), in a mixture (10 mL) of water and DMF (1:4) following our earlier report [43]. The reaction mixture was briefly mechanically agitated and immersed in a laboratory sonication bath alternatively at room temperature for 2 days. The Fc and reduced graphene oxide hybrid adduct (Fc–RGO adduct) was collected by centrifugation and washed thoroughly by several sonication and centrifugation cycles using DMF. This Fc–RGO adduct solution (~0.15 mg/mL) was then cast on the surface of the printed graphene electrode (7 mm²) produced above, and the H₂O₂ sensor was obtained after drying at 50 °C in air for 2 h.

3. Results and discussion

3.1 Ink and substrate preparation

There are many parameters involved in achieving a repeatable and reliable printing process to produce continuous and conducting patterns with high quality. Conventional pigments in inkjet inks contain particles generally in the size range 100–400 nm [44]. In the case of graphene as the base conducting filler for conducting inks, we found that restricting the size of graphene materials in the prepared inks to the above range is the key to obtaining improved image quality and printhead reliability. Thus, to have a uniform and required size of graphene sheets in the ink, the dispersed graphene solutions were first centrifuged



to remove large particles, and then the suspension was filtered through a filter with a pore size of $0.45\ \mu\text{m}$ to produce the inks. By means of a large number of AFM images, it was found that the sheet size was generally smaller than $400\ \text{nm}$ (Fig. 1). Interestingly, we found that the sheet thickness and size of the graphene sheets prepared from GO and FGO inks were very similar. One possible explanation is that the centrifugation and filtration removed the graphene sheets with larger size, particularly for the FGO ink. This would generate graphene sheets with similar sizes for the two inks. Also, sonication could possibly have caused FGO to exfoliate into GO. The inks can be stored for several months without any aggregation.

Viscosity is another important factor, which significantly affects the printing process and image quality. Because the equipment we used is a simple commercial office printer, the viscosity of the prepared ink cannot be too high in order to ensure that the patterns can be printed in a continuous form [3]. With the particular printer we used (HP Deskjet K7108), we found that

designed patterns could be printed well only when the concentration of ink made from GO (GO ink) was no more than $9\ \text{mg/mL}$, and that of ink made from FGO (FGO ink) was less than $5\ \text{mg/mL}$.

Besides the physical properties of the prepared inks, surface wettability of substrates is also a factor which significantly influences the image quality. Although patterns could be easily printed on paper with good quality, they were not continuous when printed on hydrophobic plastic substrates such as PET or PI. Thus, modification of the surface wettability of plastic substrates is particularly important for inkjet printing. Considering that graphene-based inks are hydrophilic and electrically negatively charged [45], we adopted a self-assembled polyelectrolyte technique to create a buffer zone with appropriate surface properties for printing [46, 47]. Thus, a hydrophilic buffer layer was produced by a repeated alternate dipping process using PSS and PEI as the two wetting agents. The substrate was first dipped in the anionic polyelectrolyte PSS solution and then in the

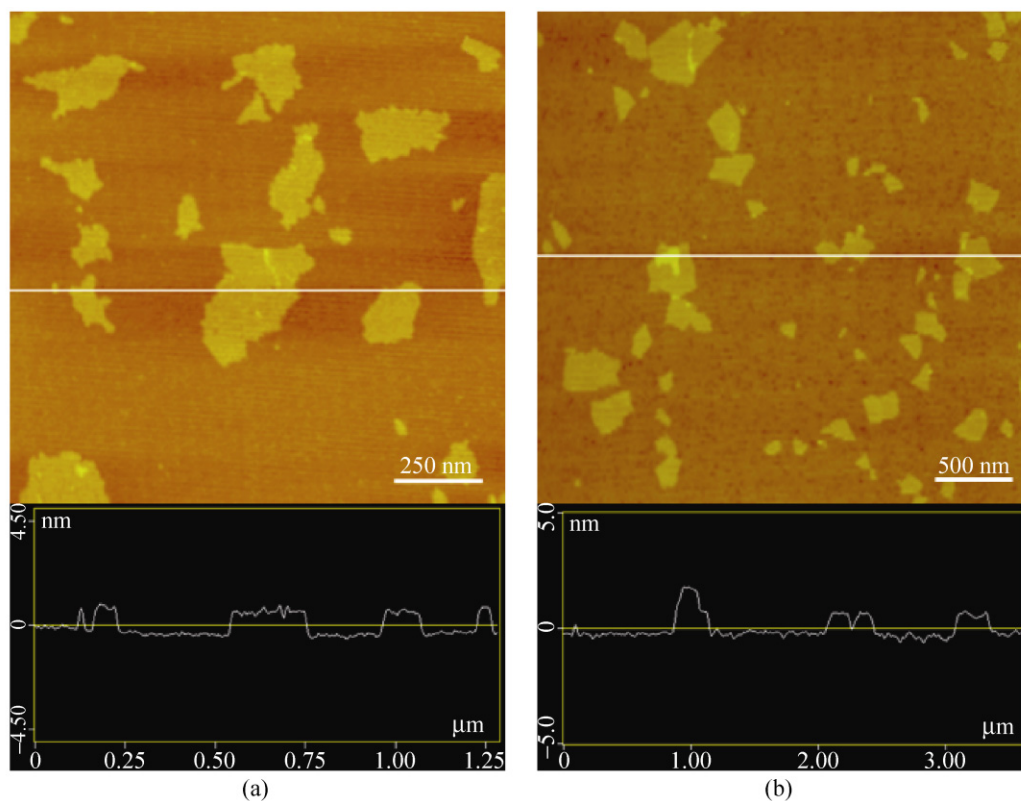


Figure 1 Typical tapping mode AFM images (top) and the corresponding height cross-sectional profiles (bottom) of (a) GO sheets in GO ink ($0.1\ \text{mg/mL}$) and (b) FGO sheets in FGO ink ($0.1\ \text{mg/mL}$) deposited on a mica substrate

cationic polyelectrolyte PEI solution. This process creates a hydrophilic buffer layer and thus changes the wetting properties of the hydrophobic substrates into hydrophilic. During this wetting process, the oppositely-charged polymers (PSS and PEI) become adsorbed onto the polymer substrate layer-by-layer. The surface wettability of the modified substrate is determined by the outermost positive polyelectrolyte PEI layer. After the surface treatment, the contact angle with the GO solution decreased from 66.5° to 26.3° . The introduction of polyelectrolyte layers generates significant improvements in the quality of the printed patterns, as shown in Fig. 2, and a variety of high quality patterns with excellent continuity and uniformity were printed on different flexible substrates such as paper, PET, and PI with the simple office inkjet printer.

3.2 Variation in conductivity as a function of the thickness of printed film/patterns

The thickness of the printed patterns can be simply controlled by printing the patterns different numbers of times (Fig. S-2 in the ESM). The relationship between the number of times and the conductivity of

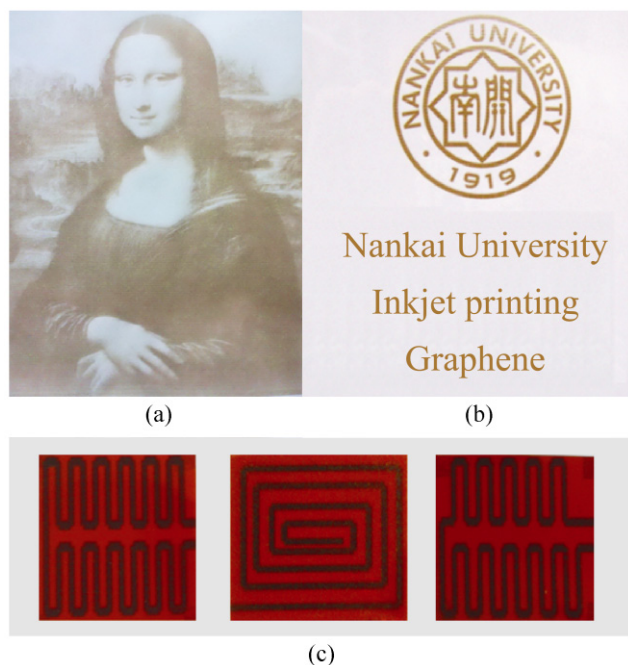


Figure 2 Different patterns printed on various substrates by using GO or FGO inks with high resolution: patterns printed (a) on normal office printing paper using FGO ink with a concentration of 5 mg/mL; (b) on PET using GO ink with a concentration of 9 mg/mL; (c) on PI using FGO ink with a concentration of 5 mg/mL.

the printed patterns on PI after reduction is illustrated in Fig. 3. As expected, the conductivity of the patterns increased as the number of times the patterns were printed increased. The morphology, as revealed by the SEM images in Fig. 4 and the AFM images in Fig. 5, featured many ridges caused by the “coffee ring effect” on the printed zone [48]. As the number of printing times increased, the number of ridges increased, and at the same time, the ridges made of graphene became thicker and better connected to each other. Although there were so many ridges in the films, the surface roughness of the films remained very low (Fig. 5). Both high conductivity and low surface roughness are important if the patterns are to be used as electrodes. Figure 3 also shows that the conductivity of patterns printed using FGO ink is higher than that printed using GO ink for the same number of printing times. Since the size and thickness of the graphene materials in the two types of inks are similar, as discussed above, this phenomenon may be attributed to the difference in the degree of functionalization of the GO and FGO. This conclusion is supported by the mass loss in TGA. The TGA trace (Fig. 6) of the FGO used in the FGO ink showed a mass loss of 21% in the range 110–230 °C, corresponding to the removal of labile oxygen-containing groups. But, in the same temperature range, the GO used in the GO ink exhibited a weight loss of about 27%. This suggests content of oxygen-containing groups in FGO is lower than that in GO. Indeed, it is expected that the

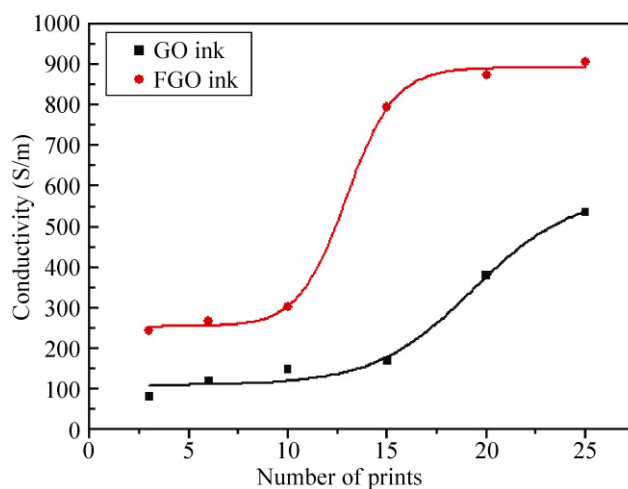


Figure 3 The relationship between the number of printing times and the electrical conductivity of the reduced patterns on PI

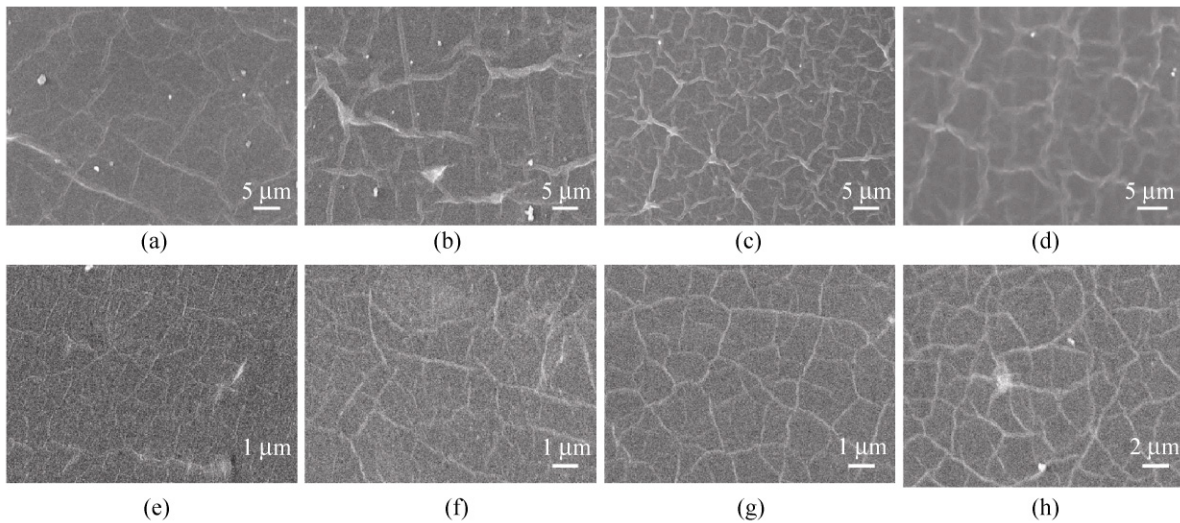


Figure 4 Scanning electron microscope images of the films printed different numbers of times on PI using GO ink and FGO ink: (a)–(d) using GO ink (6, 10, 15, and 20 times); (d)–(h) using FGO ink (6, 10, 15, and 20 times)

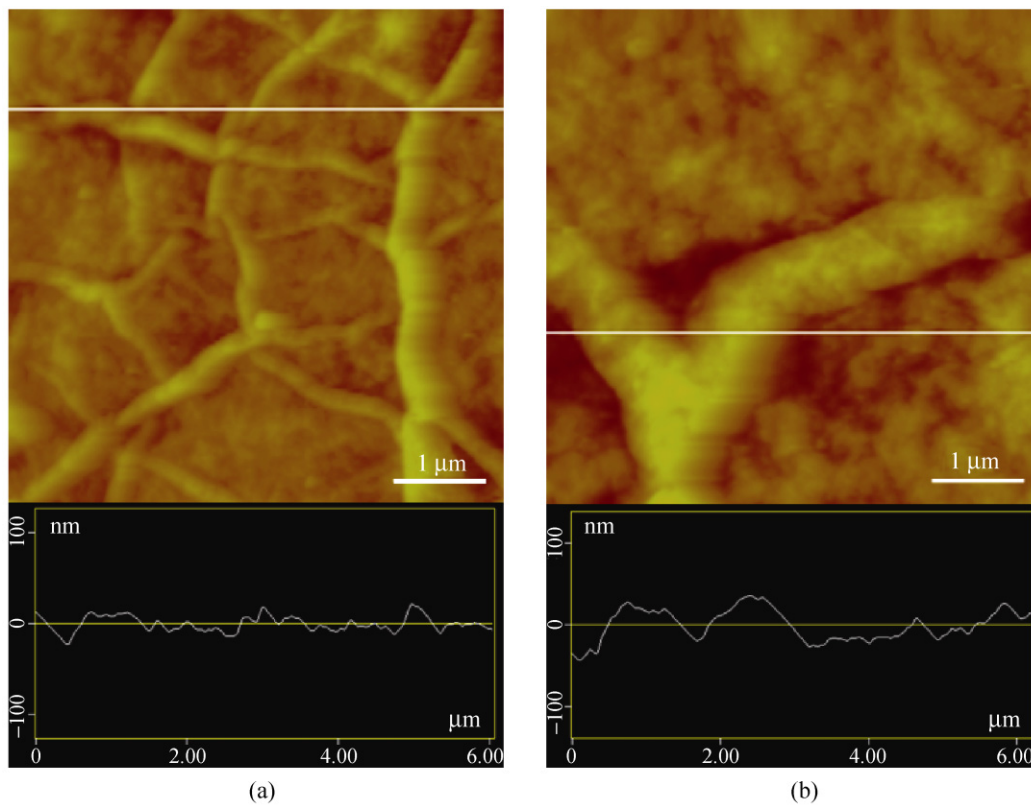


Figure 5 Surface morphology and height images of reduced patterns printed on PI: (a) the morphology of reduced patterns generated by printing 25 times using FGO ink. The surface roughness of the 1.5 μm thick pattern over a 6.2 $\mu\text{m} \times 6.2 \mu\text{m}$ area is ca. 30 nm; (b) the morphology of the reduced patterns generated by printing 25 times using GO ink. The surface roughness of the 1.8 μm thick pattern over a 6.2 $\mu\text{m} \times 6.2 \mu\text{m}$ area is ca. 60 nm

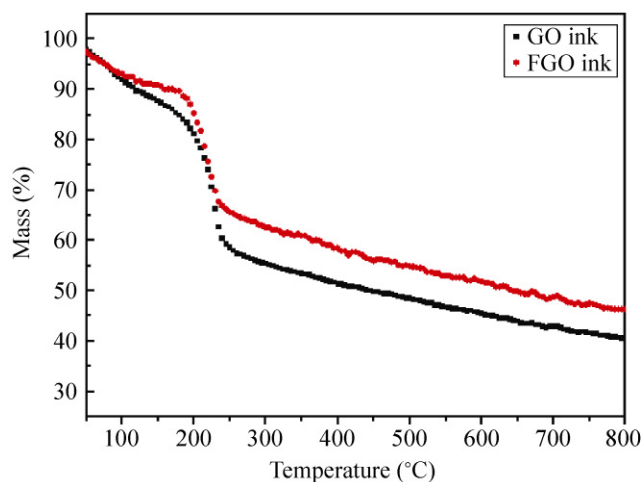


Figure 6 TGA curves of graphene oxide materials used in GO ink and FGO ink at a heating rate of 10 °C in N₂ atmosphere

graphene planes of FGO should have fewer defects due to the milder chemical process used to prepare FGO [39, 40]. Consequently, patterns printed using FGO ink showed a higher electrical conductivity than those printed using GO ink under the same printing and reduction conditions due to their higher integrity.

3.3 Flexibility of printed patterns

To demonstrate the mechanical flexibility of the graphene patterns produced using inkjet printing, we measured the conductivity of the patterns on various substrates before and after bending cycles (Fig. 7). No decrease in conductivity was observed even after hundreds of bending cycles. For example, when the

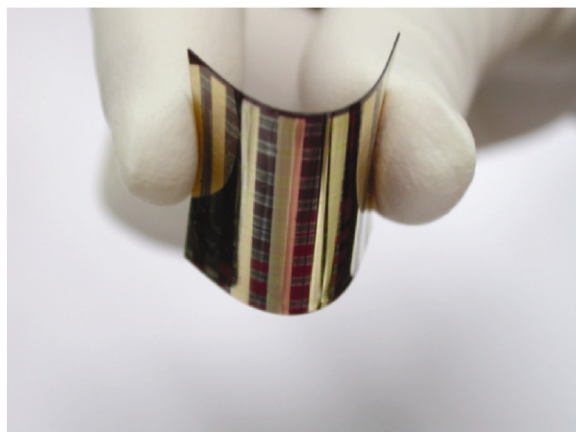


Figure 7 Photograph of a printed pattern on a PI substrate bent outwards by nearly 75°. The FGO ink printed pattern was reduced by thermal annealing

20 times-printed pattern was bent outwards by 75°, its electrical conductivity was 760 S/m. When the bending force was released after 100 bending cycles, the pattern became flat again and its conductivity returned to the same value (874 S/m) as before it was bent. Furthermore, there were no observable cracks on the graphene film. These results indicate that inkjet printing of graphene ink can produce flexible patterned electrodes with the performance required for use in flexible devices.

3.4 Device demonstration using printed graphene patterns

The excellent conductivity and flexibility of the patterns printed directly from graphene inks indicate that these patterns can be used to fabricate a variety of functional circuits and devices. We have used them to fabricate two devices as a demonstration of their practical applications. As shown in Fig. 8, the pattern printed on PI was reduced and then used to fabricate a flexible electronic circuit. The circuit was composed of a 3.0 V battery, a printed graphene electronic circuit, and an LED. The printed graphene pattern worked rather well as a normal electronic circuit connected in series with the battery and the LED. Furthermore, the brightness of the LED was identical, irrespective of whether the printed graphene electronic circuit was flat (Fig. 8(a)) or bent (Fig. 8(c)). This indicates that the printed patterns could be used as the electrode or

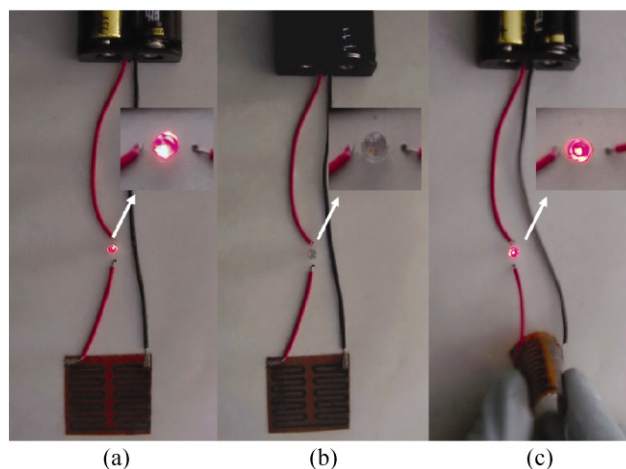


Figure 8 Photographs of flexible graphene circuits: (a) circuit with battery when the printed pattern was flat; (b) circuit without battery; (c) circuit with battery when the printed pattern was bent. Shown in the insets are the ON/OFF states of the LED under different conditions

electronic circuit in other applications such as OPVs, ultracapacitors, and lithium batteries.

In addition to producing a flexible circuit, we also used the printed graphene patterns as the working electrode to fabricate a simple enzyme-free electrochemical sensor for H_2O_2 detection. The working electrode for the sensor was fabricated using inkjet printing as above, an Ag/AgCl electrode was used as the reference electrode and a Pt wire as the auxiliary electrode. Fc-RGO adduct (Fig. S-3 and Fig. S-4 in the ESM) was used as the active material for the detection of H_2O_2 , and it was cast on the printed graphene electrode as detailed in the Experimental section. Typical cyclic voltammograms (CV) of this sensor for H_2O_2 detection in an Ar-saturated phosphate buffer solution (PBS) are shown in Fig. 9. There was a clear reduction current peak at -0.26 V associated with the H_2O_2 reduction. This reduction potential is at a much lower position than that observed with a normal bare glassy carbon electrode and similar to that in an earlier report using a hybrid glassy carbon electrode modified with a ferrocene-single-walled carbon nanotube (Fc-SWNT) adduct as a sensor [38]. In the case of the printed graphene electrode modified with RGO, a reduction peak was observed at -0.46 V . This position is similar to that observed for a bare glassy carbon electrode for H_2O_2 detection. The change in the position of the reduction peaks from -0.46 V to -0.26 V indicates the

excellent electrocatalytic properties of the Fc-RGO adduct modified electrode, which can be attributed to the cooperative effect due to the π - π stacking between Fc and RGO and the better charge transportation between the printed graphene electrode and the solution due to the presence of the Fc-RGO adduct. Compared with the widely studied H_2O_2 sensors based on enzymes immobilized on a glassy carbon electrode, our graphene-based sensor fabricated using simple inkjet printing technology has the advantages of low cost, flexibility, ease of mass fabrication and usage under harsh experimental conditions.

4. Conclusions

A simple and practical inkjet printing method for fabricating electrically conductive and flexible patterns has been demonstrated using graphene inks. Various high quality patterns can be printed on paper and plastic substrates by using both GO and FGO inks directly with a simple standard office inkjet printer. More importantly, these conductive patterns retain their high electrical conductivity even after many bending cycles. Based on these excellent properties, flexible circuits and effective electrochemical H_2O_2 sensors have been fabricated for demonstration purposes using these printed graphene patterns. The results indicate that inkjet printing using graphene-based

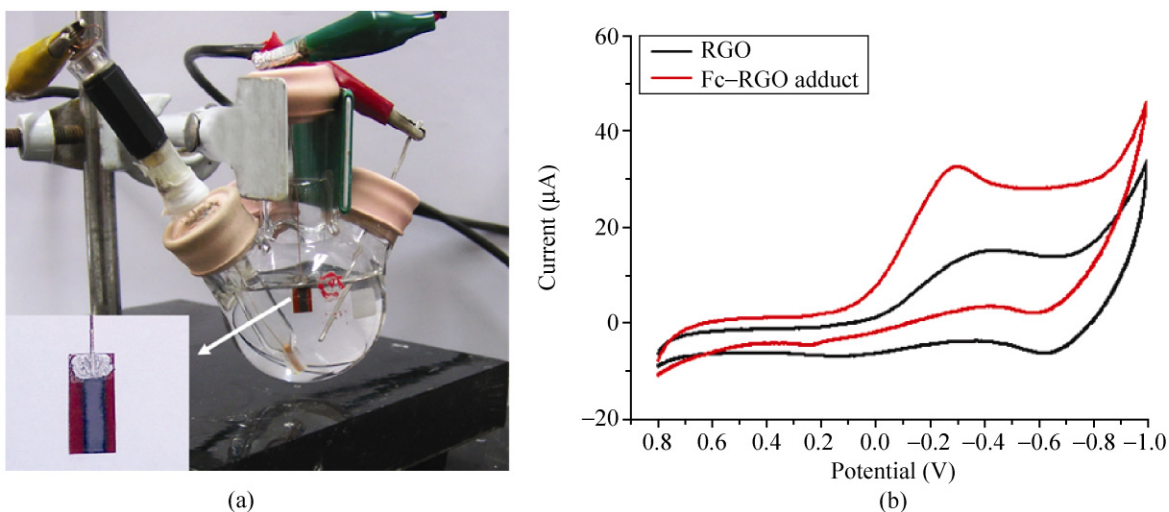


Figure 9 CV measurements of the H_2O_2 sensors. (a) The three-electrode method to detect H_2O_2 in 0.05 mol/L PBS (pH 7.4) and 0.1 mol/L KCl. Shown in the inset is a bare printed graphene electrode. (b) Cyclic voltammograms of RGO (black) and Fc-RGO adduct (red) modified printed graphene electrodes in 5 mmol/L H_2O_2 , 0.05 mol/L PBS (pH 7.4), and 0.1 mol/L KCl saturated with Ar at a 50 mV/s scan rate

inks could find wide applications in various flexible, low-cost graphene devices, such as FETs, solar cells, and displays.

Acknowledgements

The authors gratefully acknowledge financial support from the the National Natural Science Foundation of China (Grants No. 50933003, 50902073, 50903044, and 20774047), Ministry of Science and Technology of China (Grant No. 2009AA032304, 2011CB932602), Natural Science Foundation of Tianjin City (Grant No. 08JCZDJC25300).

Electronic Supplementary Material: Photograph of GO ink and FGO ink, photograph of patterns printed on PI with different printing times, Raman spectra of Fc, RGO, Fc-RGO adduct, TEM images of RGO and Fc-RGO adduct are available in the online version of this article at <http://dx.doi.org/10.1007/s12274-011-0123-z>.

References

- [1] Sele, C. W.; von Werne, T.; Friend, R. H.; Sirringhaus, H. Lithography-free, self-aligned inkjet printing with sub-hundred-nanometer resolution. *Adv. Mater.* **2005**, *17*, 997–1001.
- [2] De Gans, B. J.; Duineveld, P. C.; Schubert, U. S. Inkjet printing of polymers: State of the art and future developments. *Adv. Mater.* **2004**, *16*, 203–213.
- [3] Nur, H. M.; Song, J. H.; Evans, J. R. G.; Edirisinghe, M. J. Ink-jet printing of gold conductive tracks. *J. Mater. Sci. -Mater. El.* **2002**, *13*, 213–219.
- [4] Perelaer, J.; de Gans, B. J.; Schubert, U. S. Ink-jet printing and microwave sintering of conductive silver tracks. *Adv. Mater.* **2006**, *18*, 2101–2104.
- [5] Smith, P. J.; Shin, D. Y.; Stringer, J. E.; Derby, B.; Reis, N. Direct ink-jet printing and low temperature conversion of conductive silver patterns. *J. Mater. Sci.* **2006**, *41*, 4153–4158.
- [6] Magdassi, S.; Bassa, A.; Vinetsky, Y.; Kamysny, A. Silver nanoparticles as pigments for water-based ink-jet inks. *Chem. Mater.* **2003**, *15*, 2208–2217.
- [7] Bong, K. P.; Dongjo, K.; Sunho, J.; Jooho, M.; Jang, S. K. Direct writing of copper conductive patterns by ink-jet printing. *Thin Solid Films* **2007**, *515*, 7706–7711.
- [8] Bharathan, J.; Yang, Y. Polymer electroluminescent devices processed by inkjet printing: I. Polymer light-emitting logo. *Appl. Phys. Lett.* **1998**, *72*, 2660–2662.
- [9] Beecher, P.; Servati, P.; Rozhin, A.; Colli, A.; Scardaci, V.; Pisana, S.; Hasan, T.; Flewitt, A. J.; Robertson, J.; Hsieh, G. W., et al. Ink-jet printing of carbon nanotube thin film transistors. *J. Appl. Phys.* **2007**, *102*, 043710.
- [10] Denneulin, A.; Bras, J.; Blayo, A.; Khelifi, B.; Roussel-Dherbey, F.; Neuman, C. The influence of carbon nanotubes in inkjet printing of conductive polymer suspensions. *Nanotechnology* **2009**, *20*, 385701.
- [11] Fan, Z. J.; Wei, T.; Luo, G. H.; Wei, F. Fabrication and characterization of multi-walled carbon nanotubes-based ink. *J. Mater. Sci.* **2005**, *40*, 5075–5077.
- [12] Kordas, K.; Mustonen, T.; Toth, G.; Jantunen, H.; Lajunen, M.; Soldano, C.; Talapatra, S.; Kar, S.; Vajtai, R.; Ajayan, P. M. Inkjet printing of electrically conductive patterns of carbon nanotubes. *Small* **2006**, *2*, 1021–1025.
- [13] Song, J. W.; Yoon, Y. H.; Kim, J.; Han, C. S.; Choi, B. S.; Kim, J. H. Direct fabrication and patterning of transparent conductive carbon nanotube film using inkjet printing. In *SID International Symposium, Digest of Technical Papers, SID, Soc. Information Display: Long Beach, 2007*; pp. 1613–1616.
- [14] Panhuis, M. I. H.; Heurtematte, A.; Small, W. R.; Paunov, V. N. Inkjet printed water sensitive transparent films from natural gum-carbon nanotube composites. *Soft Matter* **2007**, *3*, 840–843.
- [15] Wei, T.; Ruan, J.; Fan, Z. J.; Luo, G. H.; Wei, F. Preparation of a carbon nanotube film by ink-jet printing. *Carbon* **2007**, *45*, 2712–2716.
- [16] Small, W. R.; Panhuis, M. I. H. Inkjet printing of transparent, electrically conducting single-walled carbon-nanotube composites. *Small* **2007**, *3*, 1500–1503.
- [17] Geim, A. K.; Novoselov, K. S. The rise of graphene. *Nat. Mater.* **2007**, *6*, 183–191.
- [18] Bunch, J. S.; van der Zande, A. M.; Verbridge, S. S.; Frank, I. W.; Tanenbaum, D. M.; Parpia, J. M.; Craighead, H. G.; McEuen, P. L. Electromechanical resonators from graphene sheets. *Science* **2007**, *315*, 490–493.
- [19] Li, D.; Kaner, R. B. Graphene-based materials. *Science* **2008**, *320*, 1170–1171.
- [20] Yan, W.; Zhiqiang, S.; Yi, H.; Yanfeng, M.; Chengyang, W.; Mingming, C.; Yongsheng, C. Supercapacitor devices based on graphene materials. *J. Phys. Chem. C* **2009**, *113*, 13103–13107.
- [21] Stoller, M. D.; Park, S. J.; Zhu, Y. W.; An, J. H.; Ruoff, R. S. Graphene-based ultracapacitors. *Nano Lett.* **2008**, *8*, 3498–3502.
- [22] Chen, Y. S.; Xu, Y. F.; Zhao, K.; Wan, X. J.; Deng, J. Ch. Towards flexible all-carbon electronics: Flexible organic field-effect transistors and inverter circuits using solution-processed all graphene source/drain/gate electrodes. *Nano Res.* **2010**, *10*, 714–721.



- [23] He, Q.; Sudibya, H. G.; Yin, Z.; Wu, S.; Li, H.; Boey, F.; Huang, W.; Chen, P.; Zhang, H. Centimeter-long and large-scale micropatterns of reduced graphene oxide films: Fabrication and sensing applications. *ACS Nano* **2010**, *4*, 3201–3208.
- [24] Wang, X.; Zhi, L. J.; Mullen, K. Transparent, conductive graphene electrodes for dye-sensitized solar cells. *Nano Lett.* **2008**, *8*, 323–327.
- [25] Junbo, W.; Becerril, H.; Zhenan, B.; Zunfeng, L.; Yongsheng, C.; Peumans, P. Organic solar cells with solution-processed graphene transparent electrodes. *Appl. Phys. Lett.* **2008**, *92*, 263302.
- [26] Xu, Y. F.; Long, G. K.; Huang, L.; Huang, Y.; Wan, X. J.; Ma, Y. F.; Chen, Y. S. Polymer photovoltaic devices with transparent graphene electrodes produced by spin-casting. *Carbon* **2010**, *48*, 3308–3311.
- [27] Liu, Q.; Liu, Z. F.; Zhong, X. Y.; Yang, L. Y.; Zhang, N.; Pan, G. L.; Yin, S. G.; Chen, Y.; Wei, J. Polymer photovoltaic cells based on solution-processable graphene and P3HT. *Adv. Funct. Mater.* **2009**, *19*, 894–904.
- [28] Yin, Z.; Sun, S.; Salim, T.; Wu, S.; Huang, X.; He, Q.; Lam, Y. M.; Zhang, H. Organic photovoltaic devices using highly flexible reduced graphene oxide films as transparent electrodes. *ACS Nano* **2010**, *4*, 5263–5268.
- [29] Fowler, J. D.; Allen, M. J.; Tung, V. C.; Yang, Y.; Kaner, R. B.; Weiller, B. H. Practical chemical sensors from chemically derived graphene. *ACS Nano* **2009**, *3*, 301–306.
- [30] Robinson, J. T.; Perkins, F. K.; Snow, E. S.; Wei, Z. Q.; Sheehan, P. E. Reduced graphene oxide molecular sensors. *Nano Lett.* **2008**, *8*, 3137–3140.
- [31] Wang, Z.; Zhou, X.; Zhang, J.; Boey, F.; Zhang, H. Direct electrochemical reduction of single-layer graphene oxide and subsequent functionalization with glucose oxidase. *J. Phys. Chem. C* **2009**, *113*, 14071–14075.
- [32] Zhou, X.; Wei, Y.; He, Q.; Boey, F.; Zhang, Q.; Zhang, H. Reduced graphene oxide films used as matrix of MALDI-TOF-MS for detection of octachlorodibenzo-*p*-dioxin. *Chem. Commun.* **2010**, *46*, 6974–6976.
- [33] Wu, J. B.; Agrawal, M.; Becerril, H. A.; Bao, Z. N.; Liu, Z. F.; Chen, Y. S.; Peumans, P. Organic light-emitting diodes on solution-processed graphene transparent electrodes. *ACS Nano* **2010**, *4*, 43–48.
- [34] Wang, S.; Ang, P. K.; Wang, Z. Q.; Tang, A. L. L.; Thong, J. T. L.; Loh, K. P. High mobility, printable, and solution-processed graphene electronics. *Nano Lett.* **2010**, *10*, 92–98.
- [35] Dua, V.; Surwade, S. P.; Ammu, S.; Agnihotra, S. R.; Jain, S.; Roberts, K. E.; Park, S.; Ruoff, R. S.; Manohar, S. K. All-organic vapor sensor using inkjet-printed reduced graphene oxide. *Angew. Chem. Int. Ed.* **2010**, *49*, 2154–2157.
- [36] Becerril, H. A.; Mao, J.; Liu, Z.; Stoltenberg, R. M.; Bao, Z.; Chen, Y. Evaluation of solution-processed reduced graphene oxide films as transparent conductors. *ACS Nano* **2008**, *2*, 463–470.
- [37] Hummers, W. S.; Offeman, R. E. Preparation of graphitic oxide. *J. Am. Chem. Soc.* **1958**, *80*, 1339.
- [38] Liu, Z. F.; Liu, Q.; Huang, Y.; Ma, Y. F.; Yin, S. G.; Zhang, X. Y.; Sun, W.; Chen, Y. S. Organic photovoltaic devices based on a novel acceptor material: Graphene. *Adv. Mater.* **2008**, *20*, 3924–3930.
- [39] Zhang, L.; Li, X.; Huang, Y.; Ma, Y. F.; Wan, X. J.; Chen, Y. S. Controlled synthesis of few-layered graphene sheets on a large scale using chemical exfoliation. *Carbon* **2010**, *48*, 2367–2371.
- [40] Long, Z.; Jiajie, L.; Yi, H.; Yanfeng, M.; Yan, W.; Yongsheng, C. Size-controlled synthesis of graphene oxide sheets on a large scale using chemical exfoliation. *Carbon* **2009**, *47*, 3365–3368.
- [41] Zhou, X.; Huang, X.; Qi, X.; Wu, S.; Xue, C.; Boey, F. Y. C.; Yan, Y.; Chen, P.; Zhang, H. *In situ* synthesis of metal nanoparticles on single-layer graphene oxide and reduced graphene oxide surfaces. *J. Phys. Chem. C* **2009**, *113*, 10842–10846.
- [42] Stankovich, S.; Dikin, D. A.; Piner, R. D.; Kohlhaas, K. A.; Kleinhammes, A.; Jia, Y.; Wu, Y.; Nguyen, S. T.; Ruoff, R. S. Synthesis of graphene-based nanosheets via chemical reduction of exfoliated graphite oxide. *Carbon* **2007**, *45*, 1558–1565.
- [43] Yang, X. Y.; Lu, Y. H.; Ma, Y. F.; Li, Y. J.; Du, F.; Chen, Y. S. Noncovalent nanohybrid of ferrocene with single-walled carbon nanotubes and its enhanced electrochemical property. *Chem. Phys. Lett.* **2006**, *420*, 416–420.
- [44] Magdassi, S.; Ben Moshe, M. Patterning of organic nanoparticles by ink-jet printing of microemulsions. *Langmuir* **2003**, *19*, 939–942.
- [45] Kim, Y. -K.; Min, D. -H. Durable large-area thin films of graphene/carbon nanotube double layers as a transparent electrode. *Langmuir* **2009**, *25*, 11302–11306.
- [46] Guo, T. F.; Chang, S. C.; Pyo, S.; Yang, Y. Vertically integrated electronic circuits via a combination of self-assembled polyelectrolytes, ink-jet printing, and electroless metal plating processes. *Langmuir* **2002**, *18*, 8142–8147.
- [47] Yoo, D.; Shiratori, S. S.; Rubner, M. F. Controlling bilayer composition and surface wettability of sequentially adsorbed multilayers of weak polyelectrolytes. *Macromolecules* **1998**, *31*, 4309–4318.
- [48] Deegan, R.; Bakajin, O.; Dupont, T.; Huber, G.; Nagel, S.; Witten, T. Capillary flow as the cause of ring stains from dried liquid drops. *Nature* **1997**, *389*, 827–829.